Journal of Zhejiang University-SCIENCE B (Biomedicine & Biotechnology) *2023 24(7):632-649*
www.jzus.zju.edu.cn; www.springer.com/journal/11585
E-mail: jzus_b@zju.edu.cn

Research Article
https://doi.org/10.1631/jzus.B2300086

Andrographolide protects against atrial fibrillation by alleviating oxidative stress injury and promoting impaired mitochondrial bioenergetics

Pengcheng YU[1*], Jiaru CAO[2*], Huaxin SUN[2], Yingchao GONG[1], Hangying YING[1], Xinyu ZHOU[1], Yuxing WANG[1], Chenyang QI[3], Hang YANG[2], Qingbo LV[1], Ling ZHANG[2✉], Xia SHENG[1✉]

[1]*Department of Cardiology, Key Laboratory of Cardiovascular Intervention and Regenerative Medicine of Zhejiang Province, Sir Run Run Shaw Hospital, Zhejiang University School of Medicine, Hangzhou 310016, China*
[2]*Xinjiang Key Laboratory of Cardiac Electrophysiology and Remodeling, the First Affiliated Hospital of Xinjiang Medical University, Urumqi 830011, China*
[3]*Department of Cardiology, the First School of Clinical Medicine of Zhejiang Chinese Medicine University, Hangzhou 310006, China*

Abstract: Atrial fibrillation (AF) is the most prevalent cardiac arrhythmia seen in clinical settings, which has been associated with substantial rates of mortality and morbidity. However, clinically available drugs have limited efficacy and adverse effects. We aimed to investigate the mechanisms of action of andrographolide (Andr) with respect to AF. We used network pharmacology approaches to investigate the possible therapeutic effect of Andr. To define the role of Andr in AF, HL-1 cells were pro-treated with Andr for 1 h before rapid electronic stimulation (RES) and rabbits were pro-treated for 1 d before rapid atrial pacing (RAP). Apoptosis, myofibril degradation, oxidative stress, and inflammation were determined. RNA sequencing (RNA-seq) was performed to investigate the relevant mechanism. Andr treatment attenuated RAP-induced atrial electrophysiological changes, inflammation, oxidative damage, and apoptosis both in vivo and in vitro. RNA-seq indicated that oxidative phosphorylation played an important role. Transmission electron microscopy and adenosine triphosphate (ATP) content assay respectively validated the morphological and functional changes in mitochondria. The translocation of nuclear factor erythroid 2-related factor 2 (Nrf2) to the nucleus and the molecular docking suggested that Andr might exert a therapeutic effect by influencing the Keap1-Nrf2 complex. In conclusions, this study revealed that Andr is a potential preventive therapeutic drug toward AF via activating the translocation of Nrf2 to the nucleus and the upregulation of heme oxygenase-1 (HO-1) to promote mitochondrial bioenergetics.

Key words: Traditional Chinese medicine; Atrial fibrillation; Andrographolide; Oxidative stress; Network pharmacology

1 Introduction

Atrial fibrillation (AF) is the most prevalent type of cardiac arrhythmia that occurs in clinical settings, which is associated with substantial rates of mortality and morbidity (Chugh et al., 2014; Chung et al., 2020). Various potential risk factors influence AF, combined with complications such as heart failure and thromboembolic events, make treatment challenging. Current managements for AF patients include drug therapy (antiarrhythmic drugs and anticoagulants) (Dobrev and Nattel, 2010) and non-pharmacological therapy (ablation) (Dobrev and Nattel, 2010; Chung et al., 2020). Drugs such as β-blockers and non-dihydropyridine calcium-channel blockers are clinically available but have some major adverse effects, including bleeding and proarrhythmic complications (Dobrev and Nattel, 2010; Amin et al., 2016). Although improvements have been made in non-pharmacological therapy, treatment effectiveness remains limited and only a proportion of AF patients respond satisfactorily (Brunner et al., 2012; Kloosterman et al., 2020; Ye et al., 2020). Traditional Chinese medicine (TCM) has been applied in Asia, especially China, for nearly 3000 years. To

✉ Xia SHENG, 3101008@zju.edu.cn
Ling ZHANG, ydzhangling@126.com
* The two authors contributed equally to this work
Xia SHENG, https://orcid.org/0000-0001-7304-7975
Ling ZHANG, https://orcid.org/0000-0002-1532-680X

Received Feb. 7, 2023; Revision accepted Apr. 9, 2023;
Crosschecked June 20, 2023

this end, some TCM formulas such as Celastrol (Ye et al., 2020), Dan hong (Zhan et al., 2023), and Suxiao Jiuxin pill (Ruan et al., 2018) have been studied in the context of cardiac research. The role of some TCMs in regulating ion channels to control cardiac rate or rhythm has been demonstrated, which indicated their potential for AF treatment (Dong et al., 2017). Moreover, clustering analysis and meta-analysis showed that TCM improves the clinical treatment efficiency of AF, increasing the success rate of conversion and shortening the conversion time (Wang et al., 2017; Lei et al., 2021).

Andrographis paniculata (Burm. F.) Nees, a well-known medicinal food, is native to Southeast Asia and grows abundantly in China, Indonesia, and Malaysia. It belongs to the Acanthaceae family and is commonly known as "King of the bitters." Andrographolide (Andr) is one of the major active constituents extracted from the traditional Chinese herb *A. paniculata*. Reports in the medical literature ascribe Andr potent actions, including anti-hyperglycemic, anti-pyretic, anti-inflammatory, anti-cancer, anti-leishmanial, fertility-boosting, anti-human immunodeficiency virus (HIV), cardiovascular, immunomodulatory, and choleretic activity (Maiti et al., 2010). More recently, there have been reports that Andr ameliorated aortic valve incrassation by inhibiting cell proliferation via the mitogen-activated protein kinase (MAPK)-extracellular signal-regulated kinase (ERK) signaling pathway (Huang et al., 2022) and alleviated aortic valve calcification by regulating lipid biosynthesis and glycerolipid metabolism or via the nuclear factor-κB (NF-κB)/serine/threonine kinase (Akt)/ERK pathway (Huang et al., 2020). In high-fat-diet-induced obese mice, Andr mitigated cardiac apoptosis to provide a cardio-protective function (Lin et al., 2020). Other research found that, through inhibiting MAPK signaling, Andr blocks the activation of cardiac fibroblasts and protects against aortic banding-induced experimental cardiac hypertrophy (Wu et al., 2017). As for myocardial infarction (MI), Andr exerted a protective effect against isoproterenol-induced MI through the inhibition of L-type Ca^{2+} channels and the increase in cardiac transient outward K^+ currents (Elasoru et al., 2021). In addition, Andr alleviated adverse cardiac remodeling following MI through the enhancement of nuclear factor erythroid 2-related factor 2 (Nrf2) signaling pathway (Xie et al., 2020). In other non-heart disease studies, by strengthening intestinal barrier function and shaping the intestinal microbial composition, Andr ameliorated glucose intolerance and insulin resistance, as well as attenuated diabetes-associated redox disturbance and inflammation in db/db diabetic mice (Su et al., 2020); in 3T3-L1 preadipocytes, via the suppression of glutathione peroxidase 1 (GPX1) and glutathione (GSH) depletion, Andr exerted a proliferation inhibitory effect (Chen et al., 2016). However, some scholars reported that by inhibiting voltage-gated Na^+, and Ca^{2+} channels, Andr ameliorated the symptoms of aconitine-induced arrhythmia in rabbits (Zeng et al., 2017), which result—the downregulation of L-type Ca^{2+} current during the development of AF—was against common sense. Hence, we speculate that the above findings might be due to the use of aconitine as an inducer or the fact that the ex vivo experiment cannot reflect the whole-body conditions. Moreover, there may be other potential mechanisms to interpret the therapeutic effect of Andr on AF.

There is scope for the treatment of complex diseases by TCM through the synergistic effects of multiple components, which affect many molecular targets in contrast to Western medicine that tends to be directed at one specific target (Ma et al., 2015). However, this complexity presents a barrier to the pharmacological and mechanistic study of some TCM examples. The development of network pharmacology approaches with access to databases provides a solution to this problem and can be instrumental in predicting the actions and effects of TCM (Hopkins, 2008). This approach has been widely applied to the study of TCM for the treatment of various diseases, such as hepatocellular carcinoma (Guo et al., 2019), heart disease (Tan et al., 2022), and coronavirus disease 2019 (COVID-19) (Li et al., 2021). There is great potential for the application of network pharmacology to orient the study of drugs and aid development. To the best of our knowledge, there have been no reports that employed network analysis to study TCM therapies relevant to AF as a distinct condition from other cardiac diseases.

In the current study, we used network databases to cross-reference potential targets with known mediators of AF to investigate the actions of Andrographis with respect to AF. Then, we tested whether Andr actually caused the therapeutic effects in AF. Our results indicated that Andr could inhibit atrial myocyte apoptosis and myolysis through the regulation of the processes of mitochondrial fission and fusion, improving

mitochondrial energy metabolism, and in turn reducing the incidence of AF.

2 Results

2.1 Results of network pharmacology analysis

Considering the similar clinical effects of both Andrographis and Andr and the fact that there are less research data on Andr, we selected Andrographis as the candidate object of network pharmacological analysis to explore the potential effects of Andr. To confirm that Andr was indeed responsible for the therapeutic effects that was obtained from the network pharmacological analysis on Andrographis, experiments on rabbits and HL-1 cells were performed.

A total of 49 components of Andrographis were obtained from the Traditional Chinese Medicine Systems Pharmacology Database and Analysis Platform (TCMSP) database (Table S1). After the absorption, distribution, metabolism and excretion (ADME) screening, 24 (48.98%) met the requirements of oral bioavailability ⩾30% and drug-likeness index ⩾0.18, which were chosen as candidate bioactive components for further analyses. A total of 294 protein targets of bioactive components present in Andrographis were retrieved from the TCMSP database (mainly from DrugBank; details are found in Table S1). After removing the duplicates, 74 protein targets were retained for further analyses. A total of 3211 human genes with relevance to AF were identified via GeneCards (Table S1). The intersection of the two target clusters yielded 51 protein targets of Andrographis components with relevance to AF (Fig. 1a).

A protein–protein interaction (PPI) network was constructed to illuminate the relationships between protein targets (Kumar et al., 2015). CytoHubba from Cytoscape was used to determine the top ten hub genes (Fig. 1b). Among these, AKT1 was identified as the most significant target with degree=41, followed by tumor necrosis factor (TNF) (degree=37), interleukin-6 (IL-6) (degree=36), heat shock protein 90α family class A member 1 (HSP90AA1) (degree=32), tumor suppressor p53 (TP53) (degree=32), caspase-3 (CASP3) (degree=32), posttranscriptional gene silencing 2 (PTGS2) (degree=31), estrogen receptor 1 (ESR1) (degree=30), c-Jun (JUN) (degree=30), and nitric oxide synthase 3 (NOS3) (degree=28).

Gene ontology (GO) and pathway enrichment analyses were performed via the functional annotation tool of the Database for Annotation, Visualization, and Integrated Discovery (DAVID) Bioinformatics Resources 6.8. A total of 203 biological process (BP), 28 cellular component (CC), and 43 molecular function (MF) terms met the criteria of count ⩾2 and expression analysis systematic explorer (EASE) score ⩽0.05 (detailed GO information is presented in Table S2). GO analysis demonstrated the involvement of these targets in response to antibiotic, extrinsic apoptotic signaling pathway in the absence of ligand, positive regulation of nitric oxide biosynthetic process, response to drug, and other BPs. Next, Kyoto Encyclopedia of Genes and Genomes (KEGG) pathway analysis was conducted (Table S2), and the top 15 significantly enriched pathways are shown in Fig. 1b. Interestingly, the top four pathways were all involved in phosphoinositide-3-kinase (PI3K)-Akt signaling and apoptosis, which ranked the 5th and 10th, respectively (Fig. 1c).

Then, a target-pathway network and a Chord plot were generated based on associated protein targets and enriched pathways. Many high-degree targets (degree⩾10) were identified to play roles in apoptosis, inflammation, and metabolism, including AKT1, phosphatidylinositol-4, 5-bisphosphate 3-kinase, catalytic subunit γ (PIK3CG), TP53, MAPK14, TNF, JUN, cyclin D1 (CCND1), protein kinase cyclic adenosine monophosphate (cAMP)-activated catalytic subunit α (PRKACA), IL-6, glycogen synthase kinase 3β (GSK3B), CASP3, cyclin-dependent kinase inhibitor 1A (CDKN1A), CASP9, C-X-C motif chemokine ligand 8 (CXCL8), calmodulin 1 (CALM1), B-cell lymphoma 2 (BCL2), CDK2, BCL2-associated X (BAX), and NOS2 (Figs. 1d and 1e).

In summary, we used network pharmacological analysis to investigate the mechanisms, by which Andrographis might treat or prevent the development and progression of AF. We concluded that components of Andrographis influence cell survival and inflammation through acting via the PI3K-Akt signaling pathway.

2.2 Effects of Andr treatment on myofibril degradation and HL-1 cell apoptosis in vitro

Oxidative stress participates in the development and perpetuation of AF and promotes atrial remodeling, both electrically and structurally (Pauklin et al., 2022). To determine a suitable drug concentration of

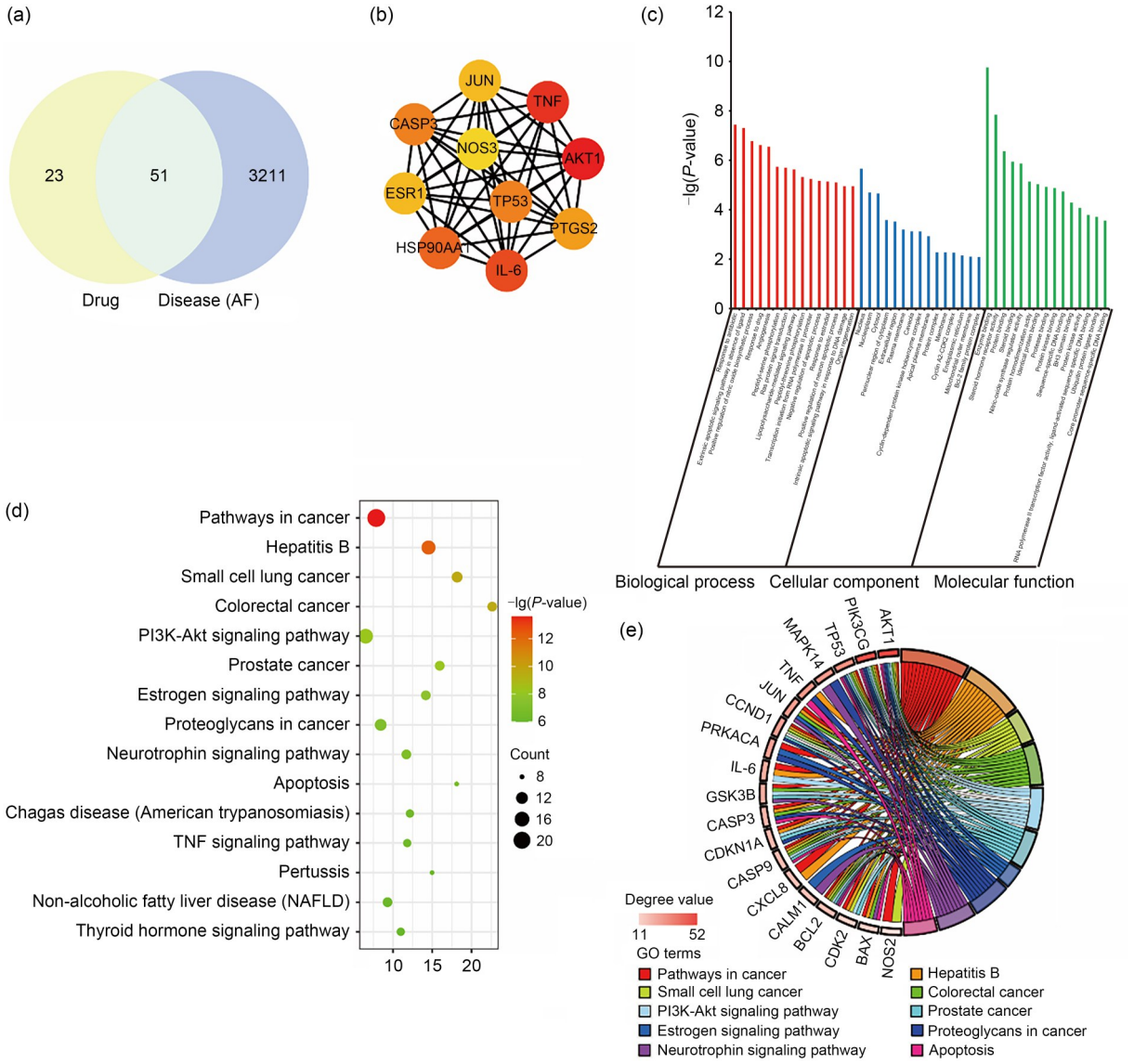

Fig. 1 Results of the network pharmacology analysis. (a) The Venn diagram was plotted by http://www.bioinformatics.com.cn, a free online platform for data analysis and visualization. The yellow circle represents the candidate targets of Andrographis on atrial fibrillation (AF). The blue one represents the AF-related genes coming from GeneCards database. (b) Protein–protein interaction (PPI) network created using STRING (http://string-db.org), and modified by the CytoHubba plug-in in Cytoscape. The scores of top ten nodes were calculated and ranked using the Maximal Clique Centrality (MCC). (c, d) Gene ontology (GO) and pathway enrichment analyses of therapy target genes of Andrographis on AF, demonstrating the top 15 biological processes (red lines), cellular components (blue lines), and molecular functions (green lines) (c) and the top 15 Kyoto Encyclopedia of Genes and Genomes (KEGG) pathways (bubble plots) (d). (e) Chord plot of the top ten KEGG enriched pathways and 19 relatively high-degree targets (degree≥10). TNF: tumor necrosis factor; IL-6: interleukin-6; HSP90AA1: heat shock protein 90α family class A member 1; TP53: tumor suppressor p53; CASP3: caspase-3; PTGS2: posttranscriptional gene silencing 2; ESR1: estrogen receptor 1; JUN: c-Jun; NOS3: nitric oxide synthase 3.

Andr, HL-1 cells were counted using the cell counting kit-8 (CCK8). We tested suitable stimulation frequencies of 0.5, 1, 3, and 5 Hz, and found that both RNA and protein levels responded the most to the 5 Hz signal based on the degradation of L-type calcium channel (LCC), considered as the marker of the successful AF model building (Figs. S1a and S1b). In addition, the dihydroethidium (DHE) staining showed that rapid electronic stimulation (RES) promoted the intracellular reactive oxygen species (ROS) level (Fig. S1c). Thus, we selected 5 Hz, 10 V, and 24 h as our model parameters.

Significant cytotoxicity was observed when using 50 μmol/L Andr to treat HL-1 cells for 24 h. Reducing Andr to 25 μmol/L alleviated the cytotoxicity and was selected as the optimal concentration (Fig. 2a). Myofibril degradation is a characteristic of atrial structural remodeling resulting from increased intracellular ROS. Heme oxygenase-1 (*HO-1*), a powerful anti-oxidative stress gene, plays an important role in AF. Different concentrations of Andr protected the degradation of cardiac troponin I (cTnI) after RES for 24 h (Fig. 2b). The optimal concentration of Andr was confirmed to be 25 μmol/L. Similar results were observed in the

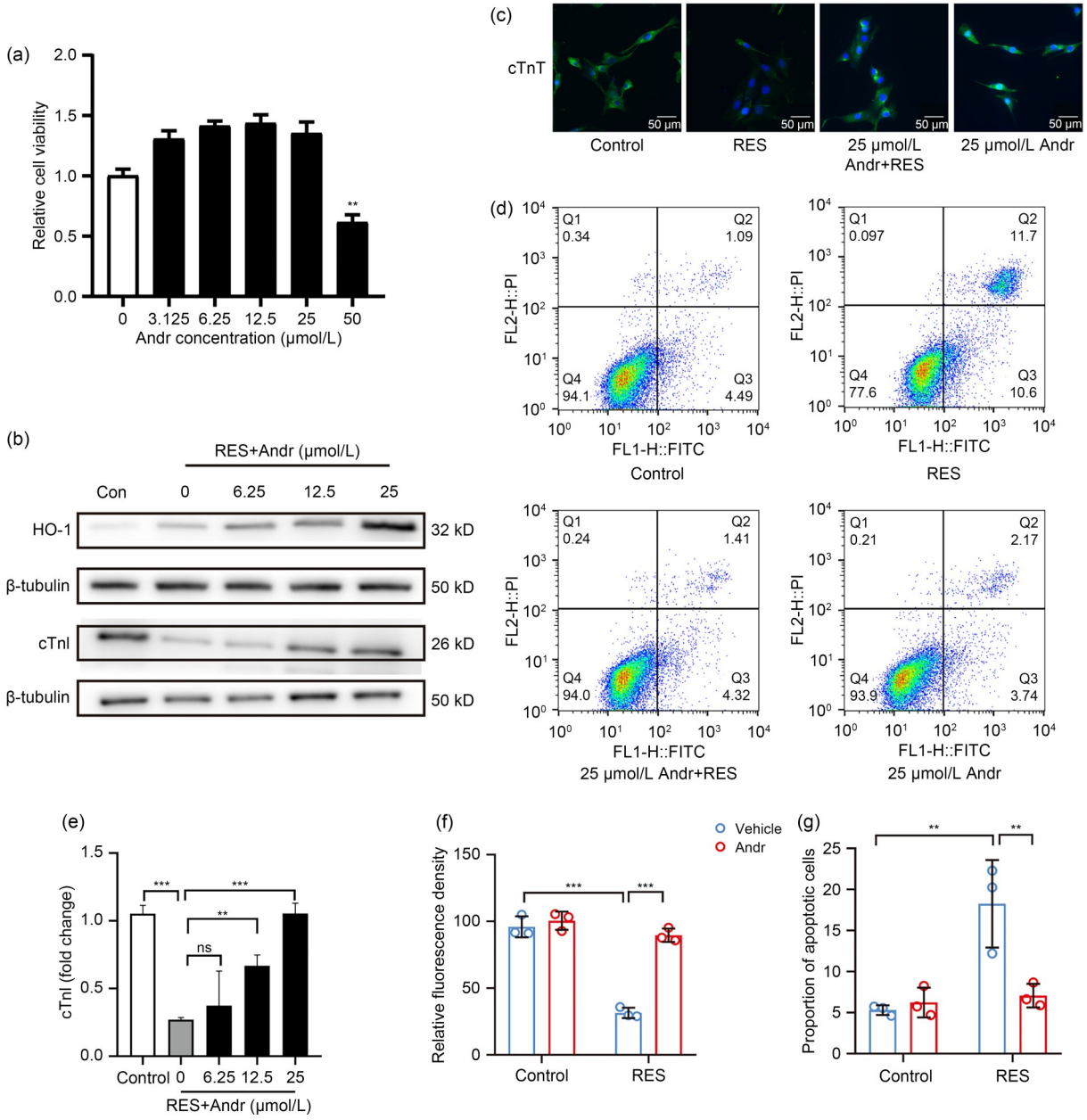

Fig. 2 Effects of andrographolide (Andr) treatment on myofibril degradation and HL-1 cell apoptosis in vitro. (a) Cell viability was accessed by the cell counting kit-8 assay. (b) Representative blots of heme oxygenase-1 (HO-1) and cardiac troponin I (cTnI). (c) Immunofluorescence staining of cTnT. (d) Representative images of fluoresceine isothiocyanate (FITC)-Annexin V/propidium iodide (PI)-positive apoptotic HL-1 cells with or without Andr treatment after rapid electronic stimulation (RES) (5 Hz, 10 V) for 24 h determined by flow cytometry. (e) Quantitative analysis of the expression of cTnI. (f) Quantitative analysis of the fluorescence density of cTnT. (g) Quantitative analysis of the proportion of apoptotic HL-1 cells. Data are expressed as mean±standard deviation (SD) (n=3). ** P<0.01, *** P<0.001; ns: not significant.

immunofluorescence assay of cardiac troponin T (cTnT) (Fig. 2c). The HO-1 levels slightly increased after RES for 24 h via the upregulation of redox balance. Perhaps more remarkably, HO-1 showed an increase dependent on Andr concentration (Fig. 2b). The DHE staining showed that RES promoted the intracellular ROS level, which could be reversed by the use of Andr (Figs. 3a and 3b).

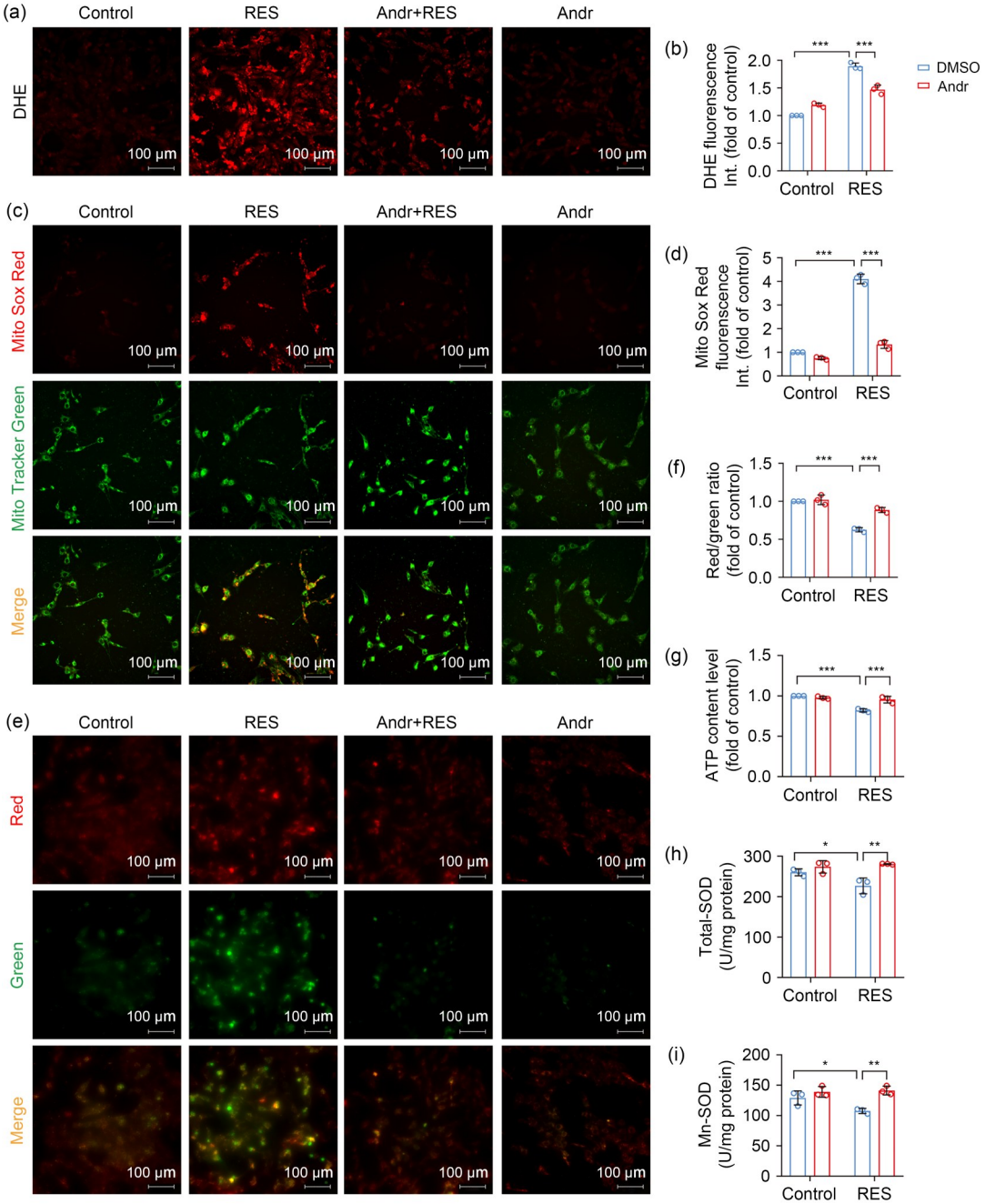

Fig. 3 Effect of andrographolide (Andr) treatment on oxidative stress injury in vitro. (a, b) Representative images and quantitative analysis of superoxide production measured by dihydroethidium (DHE) fluorescence. (c, d) Representative images and quantitative analysis of mitochondrial reactive oxygen species (ROS) stained by Mito Sox Red. (e, f) Representative images and quantitative analysis of JC-1 mitochondrial membrane potential (MMP) assay. (g) Effects of Andr treatment on the content of adenosine triphosphate (ATP) in HL-1 cells. (h, i) Effects of Andr treatment on the levels of oxidative stress markers total-superoxide dismutase (SOD) and Mn-SOD in HL-1 cells. Data are expressed as mean±standard deviation (SD) (n=3). * P<0.05, ** P<0.01, *** P<0.001. RES: rapid electronic stimulation; DMSO: dimethyl sulfoxide.

Next, we compared the ROS levels within the cell. Compared with total cellular ROS, the levels of mitochondrial ROS were similar (Figs. 3c and 3d). These results were confirmed by the JC-1 mitochondrial membrane potential (MMP) assay (Figs. 3e and 3f). As mitochondria are the major organelles for adenosine triphosphate (ATP) production and the content of cellular ATP can effectively reflect mitochondrial function, we determined the cellular ATP content. We found that Andr could promote the content of cellular ATP, which was downregulated by RES (Fig. 3g). The activity of total-superoxide dismutase (SOD) and Mn-SOD, two key enzymes in oxidative stress control, was reduced by RES, and Andr treatment effectively restored the enzyme activity (Figs. 3h and 3i).

2.3 Effect of Andr treatment on RAP-induced atrial electrophysiological changes in vivo

The results of electrophysiological examination revealed that rapid atrial pacing (RAP) for 6 h decreased the heart rate by 24.51% (sham group) vs. 20.01% (Andr group) (Figs. 4a and 4c). These findings are in line with previous reports, indicating that the construction of acute rabbit AF model was successful (Zhang et al., 2015). Compared with the sham group, the AF inducibility and duration were significantly increased in the AF group, while the stimulus thresholds were markedly declined. However, the changes above could be reversed by Andr treatment (Figs. 4b, 4d–4f). After 6 h of RAP, atrial effective refractory period (AERP) was slightly reduced in the AF group compared with the sham group at baseline; meanwhile, the window of vulnerability (WOV) increased, which could be reversed by the use of Andr (Figs. 4g and 4h).

The analysis of echocardiography and hemodynamic parameters indicated that cardiac function was not impaired after 6 h of RAP (Fig. 5a). No statistically significant difference was found in left ventricular ejection fraction (LVEF), left ventricular fractional shortening (LVFS), left atrial (LA) diameter, interventricular septal thickness at diastole (IVSd), left ventricular posterior wall at systole (LVPWs), or left ventricular posterior wall at diastole (LVPWd) (Figs. 5b–5d, 5i–5k). However, left ventricular internal dimension at systole (LVIDs), left ventricular internal dimension at diastole (LVIDd), and interventricular septal thickness at systole (IVSs) were reduced after 6 h of RAP. Regardless of RAP for 6 h, the right atrial (RA) diameter slightly increased in the Andr treatment group (Fig. 5e). Finally, Andr significantly alleviated cardiac dysfunction caused by RAP (Figs. 5f–5h).

2.4 Effect of Andr treatment on RAP-induced atrial inflammation in vivo

As reported previously, inflammation plays an important role in AF (Wang et al., 2022). Herein, the results of network pharmacological analysis also indicated the effect of Andr in anti-inflammatory processes. We next measured the inflammatory response in the RA tissue and serum of each group. Based on immunofluorescence, compared to the sham rabbit, the atrial tissue of the RAP group was positive for TNF-α. As expected, Andr treatment prevented the atrial tissue from accumulating TNF-α expression (Fig. 6a). Similar results were observed in the enzyme-linked immunosorbent assay (ELISA) of TNF-α (Fig. 6b). Additionally, the messenger RNA (mRNA) levels of the pro-inflammation-related genes *TNF-α* (Fig. 6c) and *IL-1β* (Fig. 6d) were validated by quantitative real-time polymerase chain reaction (qPCR).

2.5 Effect of Andr treatment on the atrial structural remodeling in vivo and in vitro

In addition to inflammation, atrial structural remodeling is regarded as highly important to the development of AF, mainly including fibrosis and atrial myocardial apoptosis (Wang et al., 2022). Masson staining and Sirius Red staining showed that the atrial tissue of RAP group presented no significant fibrosis (Fig. 7a). Atrial myocardial damage triggered by 6 h of RAP was confirmed by hematoxylin-eosin (HE) staining (Fig. 7b). In the RAP group, cell degeneration, an uneven distribution of cytoplasm, and local rupture of myocardial fibers were observed. Upon terminal deoxynucleotidyl transferase deoxyuridine triphosphate (dUTP) nick-end labeling (TUNEL) staining of the atrial tissue, a significantly larger number of TUNEL positive cells were detected in the RAP group compared with the sham group (Fig. 7c). In conjunction to these tests, we performed an Annexin V/propidium iodide (PI) assay to validate the effect of Andr on apoptosis (Figs. 2d and 2g).

2.6 Effect of Andr treatment on oxidative stress injury in vivo

We employed DHE staining to measure the intracellular ROS levels in rabbit tissues. RAP-induced ROS

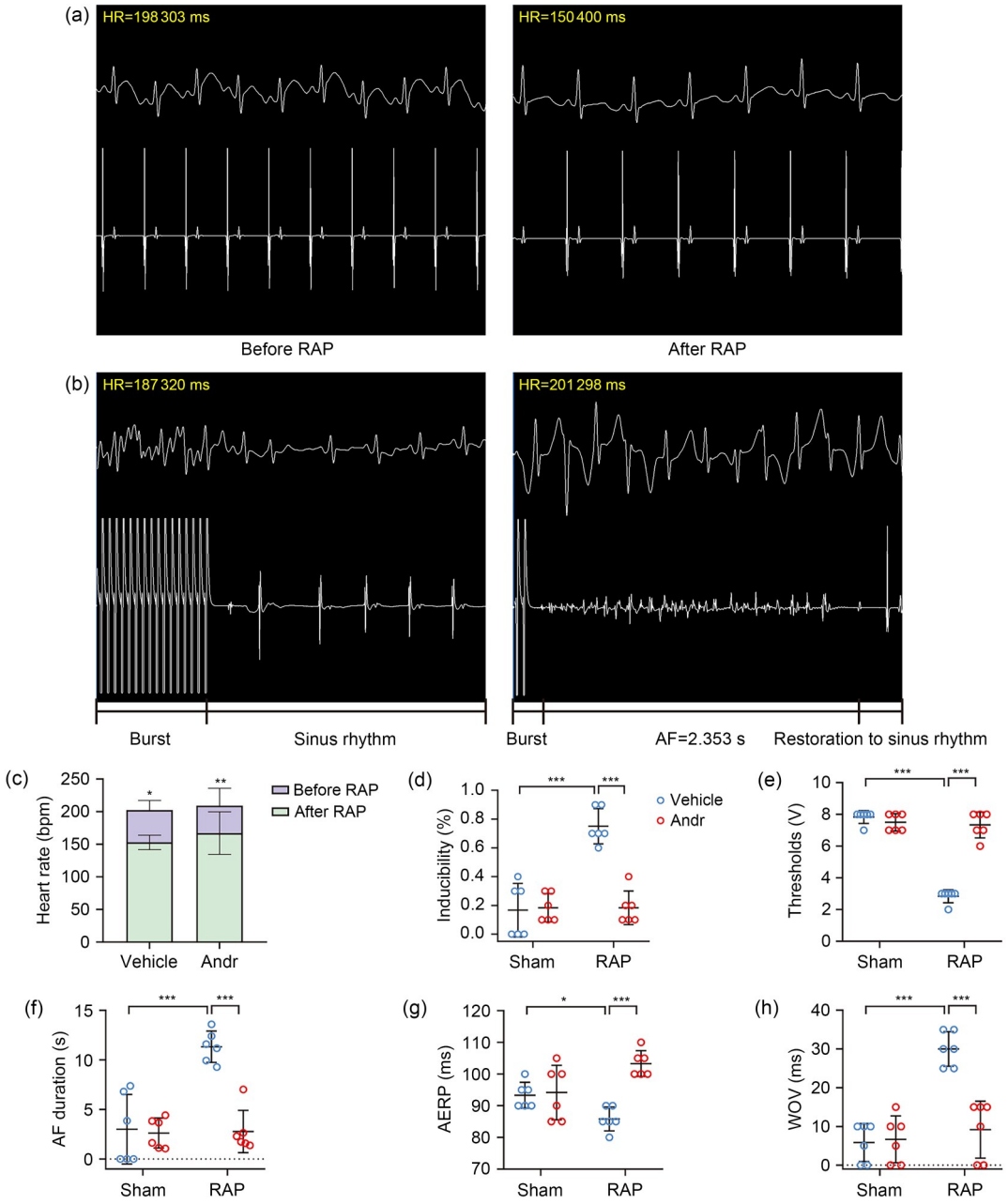

Fig. 4 Effect of andrographolide (Andr) treatment on RAP-induced atrial electrophysiological changes in vivo. (a) Representative simultaneous recordings of surface ECG (lead II) and intracardiac electrograms in rabbits before RAP (left) and after RAP (right). (b) Representative simultaneous recordings of surface ECG (lead II) and intracardiac electrograms in rabbits with (left) or without (right) successfully induced AF. (c) Quantification of heart rate before and after RAP. (d) Incidence of pacing-induced AF in rabbits. (e) Thresholds of pacing-induced AF in rabbits. The thresholds were defined as the minimum stimulation voltage that could induce AF. (f) Durations of pacing-induced AF in rabbits. The AF durations were defined as the total duration of ten successfully induced AF durations. (g) AERP of pacing-induced AF in rabbits. (h) WOV of pacing-induced AF in rabbits. Data are expressed as mean±SD (n=6). * P<0.05, ** P<0.01, *** P< 0.001. RAP: rapid atrial pacing; ECG: electrocardiogram; bpm: beats per minute; AF: atrial fibrillation; AERP: atrial effective refractory period; WOV: window of vulnerability; SD: standard deviation.

production was significantly reduced in the Andr treatment group (Fig. 8a). The immunofluorescent staining of atrial sections showed that the expression levels of cTnT and HO-1 were dramatically reduced after RAP 6 h, which could be restored by Andr treatment (Fig. 8b). Additionally, the mRNA levels of the antioxidant-related

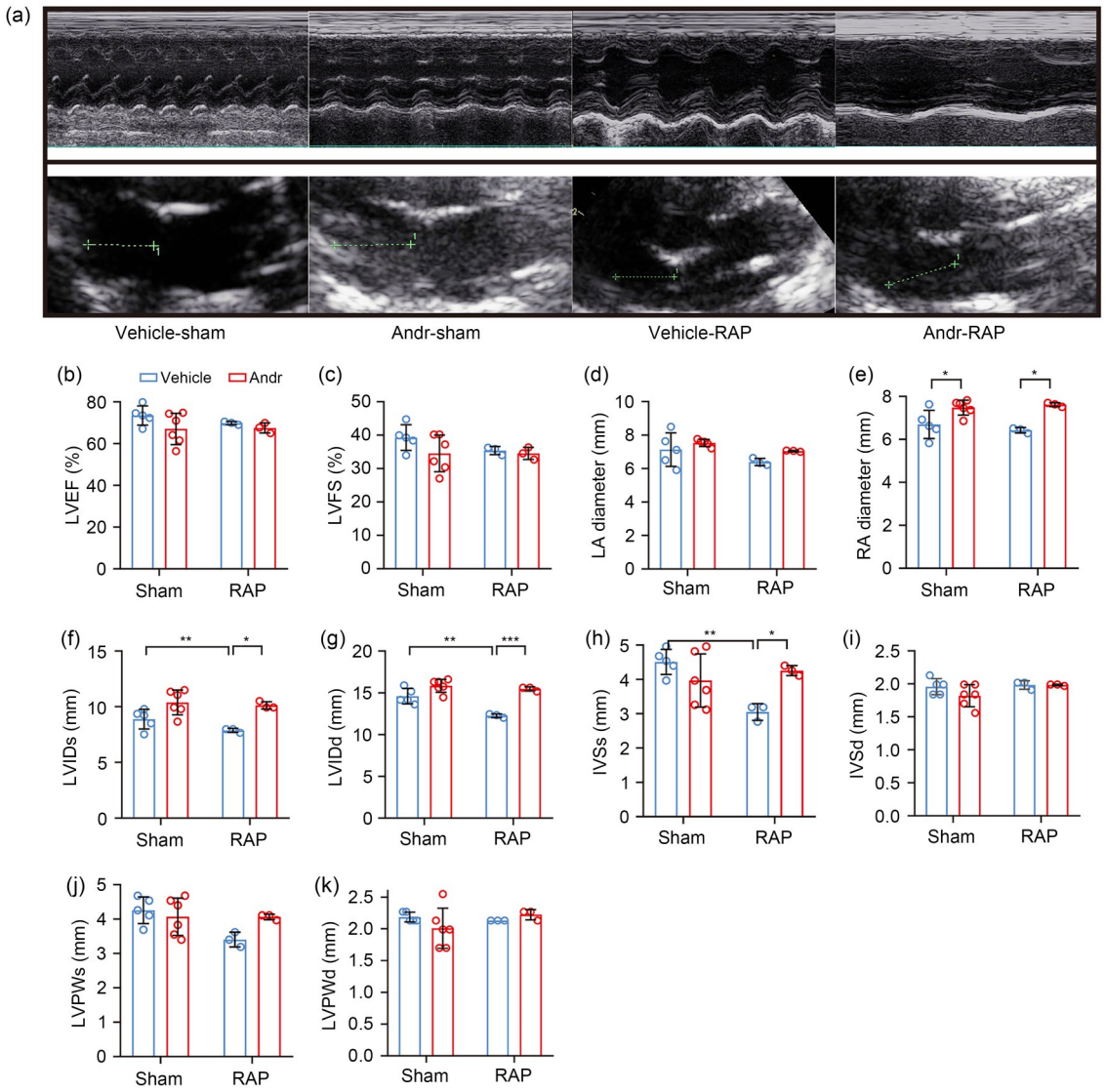

Fig. 5 Effects of andrographolide (Andr) on echocardiography in RAP-induced AF rabbits. (a) Representative 2D and M-mode echocardiographic images. (b–k) The analysis results of LVEF (b), LVFS (c), LA diameter (d), RA diameter (e), LVIDs (f), LVIDd (g), IVSs (h), IVSd (i), LVPWs (j), and LVPWd (k). Data are expressed as mean±SD (sham group, *n*=6; RAP group, *n*=3). * *P*<0.05, ** *P*<0.01, * *P*<0.001. RAP: rapid atrial pacing; AF: atrial fibrillation; 2D: two-dimensional; LVEF: left ventricular ejection fraction; LVFS: left ventricular fractional shortening; LA: left atrial; RA: right atrial; LVIDs: left ventricular internal dimension at systole; LVIDd: left ventricular internal dimension at diastole; IVSs: interventricular septal thickness at systole; IVSd: interventricular septal thickness at diastole; LVPWs: left ventricular posterior wall at systole; LVPWd: left ventricular posterior wall at diastole.**

genes NAD(P)H quinone oxidoreductase 1 (*NQO1*) (Fig. 8c), *Nrf2* (Fig. 8d), *SOD1* (Fig. 8e), and *SOD2* (Fig. 8f) were validated by qPCR in rabbit tissue.

2.7 Effect of Andr on RAP/RES, inducing atrial myocardial injury by restoring mitochondrial bioenergetics

Next, RNA sequencing (RNA-seq) was performed to further explore the pathways and mechanisms, by which Andr inhibited the changes mentioned above. We found 716 upregulated and 745 downregulated differentially expressed genes (DEGs; defined using $|\log_2(\text{fold change})|>1.5$ and *P*.adj<0.05) (Figs. 9a and 9b). Comparative GO analysis and gene set enrichment analysis (GSEA) indicated that these DEGs were significantly enriched for the generation of precursor metabolites and energy, mitochondrial protein complex, and mitochondrial membrane (Figs. 9c and 9e).

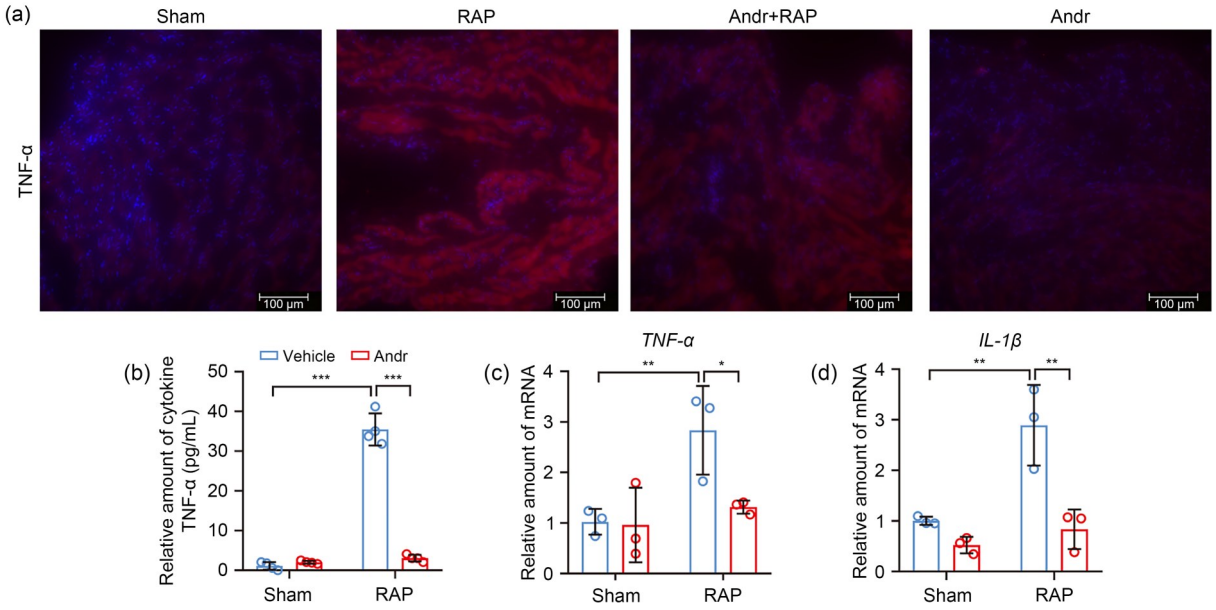

Fig. 6 Effects of andrographolide (Andr) treatment on RAP-induced atrial inflammation in vivo. (a) Representative images of anti-TNF-α staining in the atrial tissue of each group. (b) TNF-α levels in rabbits' serum determined by ELISA, *n*=4. (c, d) qPCR was used to determine the mRNA levels of *TNF-α* (c) and *IL-1β* (d) (data were normalized to *GAPDH*, *n*=3). Data are expressed as mean±SD. * *P*<0.05, ** *P*<0.01, * *P*<0.001. RAP: rapid atrial pacing; TNF-α: tumor necrosis factor-α; ELISA: enzyme-linked immunosorbent assay; qPCR: quantitative real-time polymerase chain reaction; mRNA: messenger RNA; *IL-1β*: interleukin-1β; *GAPDH*: glyceraldehyde-3-phosphate dehydrogenase; SD: standard deviation.**

Comparative KEGG pathway analysis and GSEA revealed that, apart from the top enriched KEGG pathway, several signaling pathways identified support the conclusions suggested by our data and those found from the network pharmacological analysis results. These include oxidative phosphorylation, MAPK signaling pathway, TNF signaling pathway, and PI3K-Akt signaling pathway (Figs. 9d and 9e).

Subsequently, we selected the genes of electron transport chain (ETC) complex subunits from our RNA-seq results and found that the expression of ETC complex genes was markedly upregulated in the Andr group compared to the RES group (Fig. 10a). These genes were strongly correlated with mitochondrial abnormalities. Next, we used transmission electron microscopy to observe potential phenotypic mitochondrial abnormalities in vivo. After RAP for 6 h, we observed abnormal mitochondrial morphology, mitochondrial size, aberrant cristae, and changes in the matrix color. Conversely, these abnormalities were absent in the Andr treatment group (Figs. 10b and 10d). We then assessed the expression levels. However, we did not detect the obvious change of the protein expression of ETC complex as the RNA-seq results in vitro (Fig. 10c).

As previously reported, Andr might exert an effect by the nuclear translocation of Nrf2 (Xie et al., 2020). Thus, we tested the effect of Andr on Nrf2-Keap1 complex formation in HL-1 cells. Immunofluorescence staining revealed that Andr induced the nuclear translocation of Nrf2, the main transcription factor for HO-1 and NQO1 (Fig. 11a). To predict the binding position of Andr on the Nrf2-Keap1 complex domain, AutoDock was used for 50 docking times (Figs. 11b–11d), and the binding energy of 50 docking times was presented in Table S3.

3 Discussion

AF, as one of the most common types of arrhythmias, is often accompanied with a variety of risk factors and complications. Without effective therapies that are readily or widely available in clinical practice, the increased clinical incidence and subsequent mortality associated with complicated treatments have resulted in a heavy medical burden. Therefore, it is important to discover and test new treatment strategies. During its 3000 years of history, TCM has produced unusually brilliant medicines such as artemisinin and celastrol.

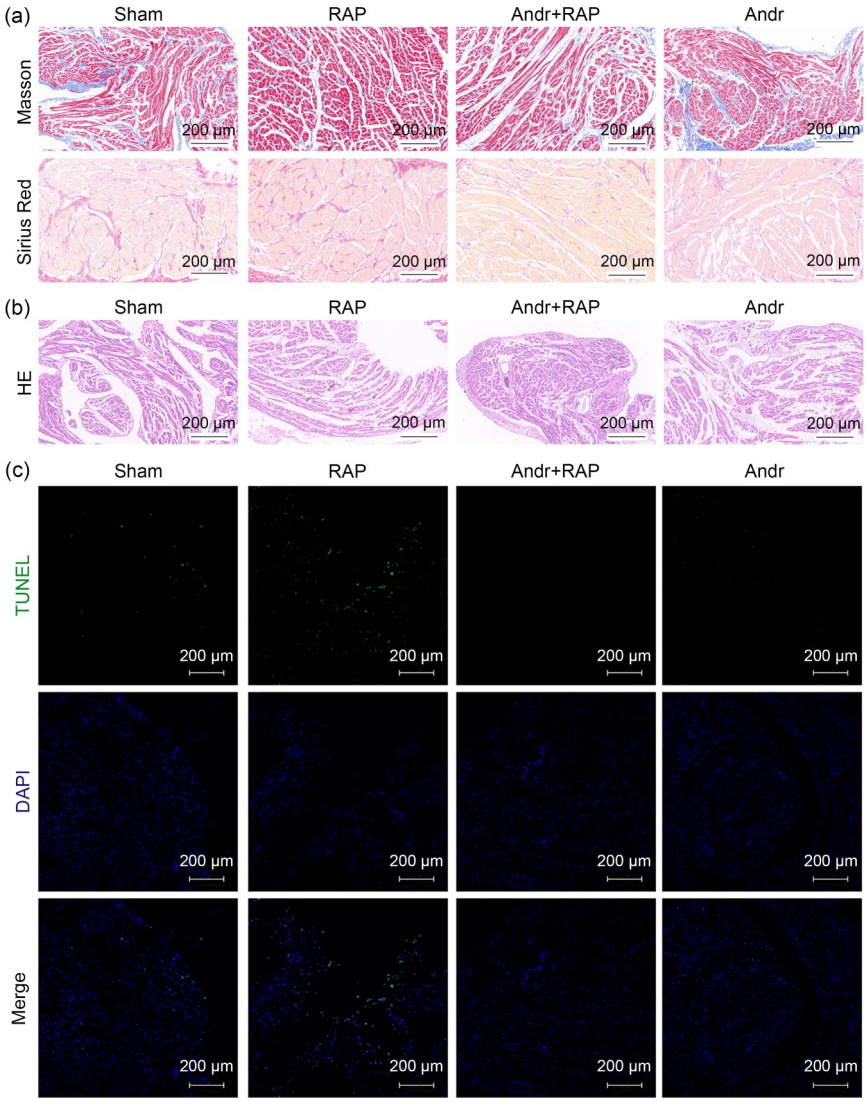

Fig. 7 Effects of andrographolide (Andr) treatment on the atrial structural remodeling in vivo. (a) Representative images of Masson staining and Sirius Red staining. (b) Representative images of hematoxylin-eosin (HE) staining. (c) Representative images of terminal deoxynucleotidyl transferase deoxyuridine triphosphate (dUTP) nick-end labeling (TUNEL). RAP: rapid atrial pacing; DAPI: 4',6-diamidino-2-phenylindole.

Recently, a widespread concern surrounding the pharmacological actions of Andr has surfaced. Considering the high cost and difficulties of constructing AF animal models, we took a pharmacological approach to investigate the possible therapeutic effect of Andrographis on AF, with the aim to provide future research directions. Andrographis was selected instead of Andr due to a lack of published data on the latter. The existing mass spectrometry results for Andrographis suggested similar clinical uses for the two. Our data indicated that cell survival and anti-oxidative stress might be the main target of the drug, possibly through modulation of PI3K-Akt signaling pathway and binding to the Nrf2-Keap1 complex to regulate the nuclear translocation of Nrf2.

Previous studies indicated that Andr ameliorates the symptoms of aconitine-induced arrhythmia in rabbits by inhibiting Ca^{2+} channels. In this study, we validated the therapeutic effect of Andr on AF and explored the possible underlying mechanism by establishing acute AF models at three different levels: molecular, cellular, and systemic. RAP treatment for 6 h significantly reduced the AF-induced threshold, increased the AF inducibility and duration, shortened AERP, and lengthened WOV. These results were similar to the aforementioned report and marked the success of building

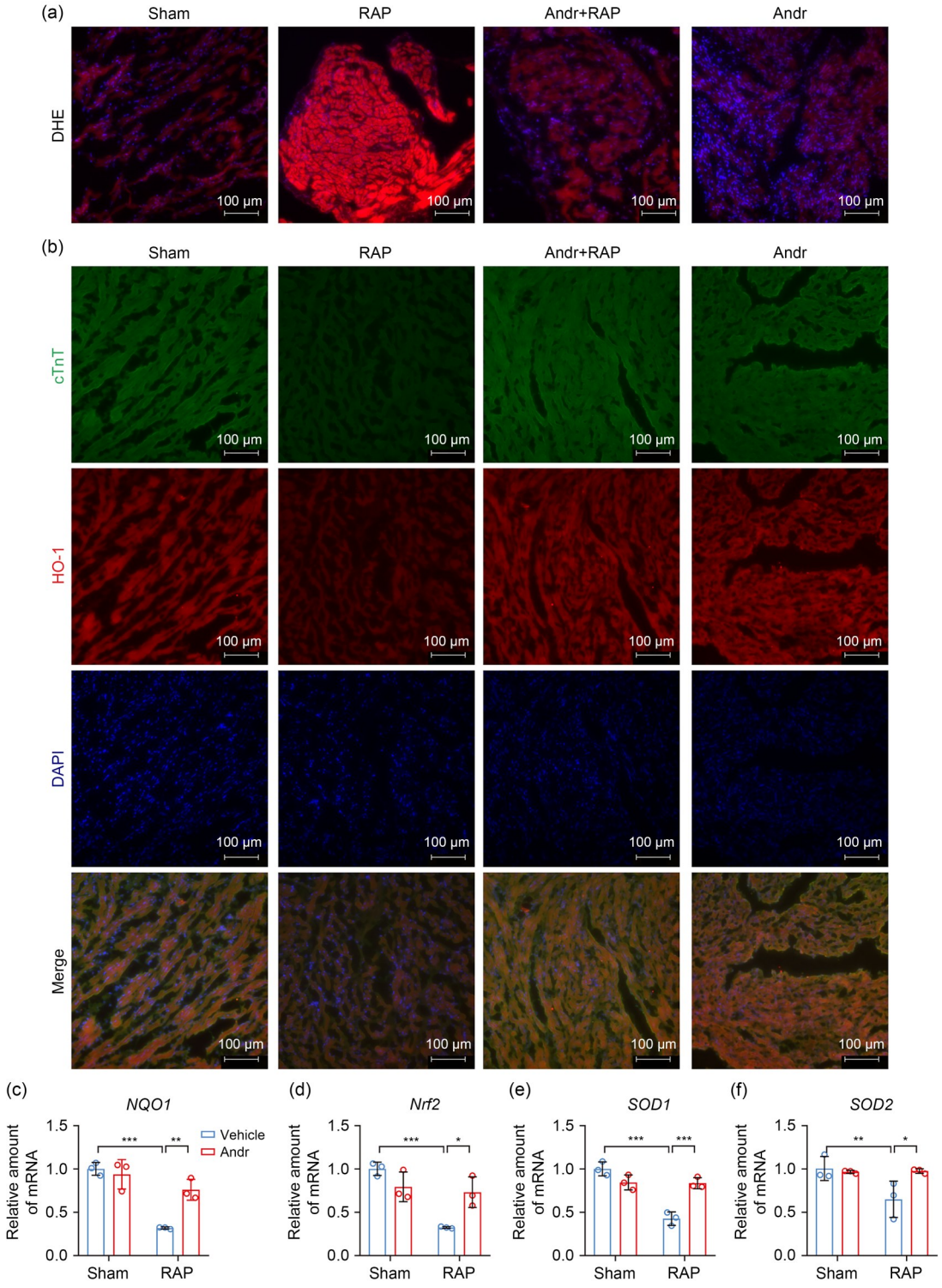

Fig. 8 Effect of andrographolide (Andr) treatment on oxidative stress injury in vivo. (a) Representative dihydroethidium (DHE) fluorescence images of superoxide production in rabbits. (b) Representative images of cardiac troponin T (cTnT) and heme oxygenase-1 (HO-1) staining in the atrial of each group. (c–f) qPCR was carried out to determine the mRNA levels of *NQO1* (c), *Nrf2* (d), *SOD1* (e), and *SOD2* (f) (data were normalized to *GAPDH*). Data are expressed as mean±SD (*n*=3). * *P*<0.05, ** *P*<0.01, * *P*<0.001. RAP: rapid atrial pacing; qPCR: quantitative real-time polymerase chain reaction; *NQO1*: NAD(P)H quinone oxidoreductase 1; *Nrf2*: nuclear factor erythroid 2-related factor 2; *SOD*: superoxide dismutase; *GAPDH*: glyceraldehyde-3-phosphate dehydrogenase; DAPI: 4',6-diamidino-2-phenylindole; SD: standard deviation.**

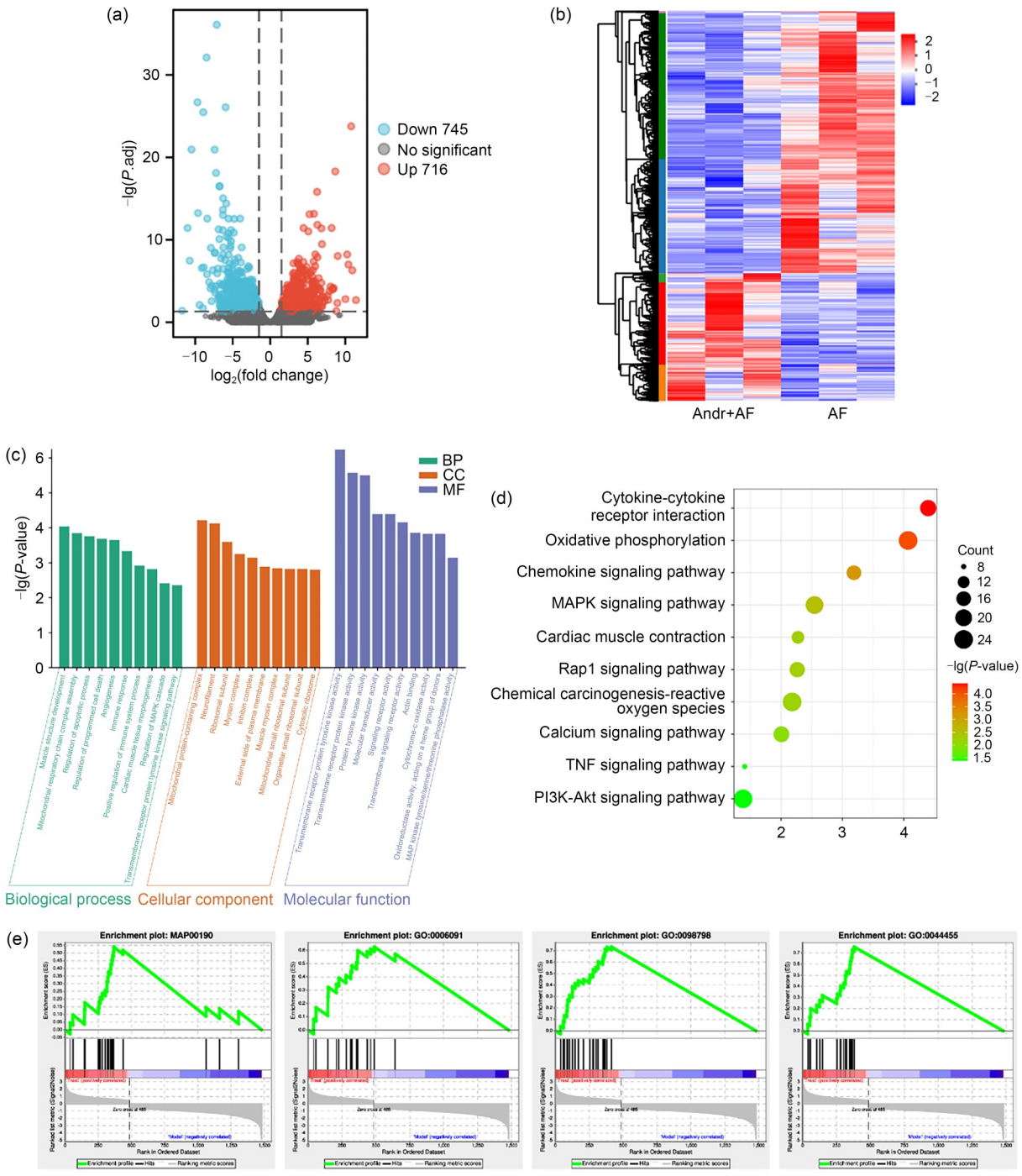

Fig. 9 Protective effect of andrographolide (Andr) through regulating the mitochondria. (a) Volcano plots displaying the expression of DEGs between the AF and AF+Andr groups. (b) Heatmap of the DEGs between the RAP and Andr+RAP groups. (c, d) GO and KEGG pathway analyses plotted using the online tool at http://www.bioinformatics.com.cn. (e) GSEA analysis results. DEG: differentially expressed gene; AF: atrial fibrillation; RAP: rapid atrial pacing; GO: gene ontology; KEGG: Kyoto Encyclopedia of Genes and Genomes; GSEA: gene set enrichment analysis; BP: biological process; CC: cellular component; MF: molecular function; MAPK: mitogen-activated protein kinase; TNF: tumor necrosis factor; PI3K: phosphoinositide-3-kinase; Akt: serine/threonine kinase.

the acute AF rabbit model. To validate the action of Andr on AF in rabbits, Andr was injected (10 mg/kg, intraperitoneally) one day before RAP. As expected, Andr treatment inhibited the RAP-induced threshold

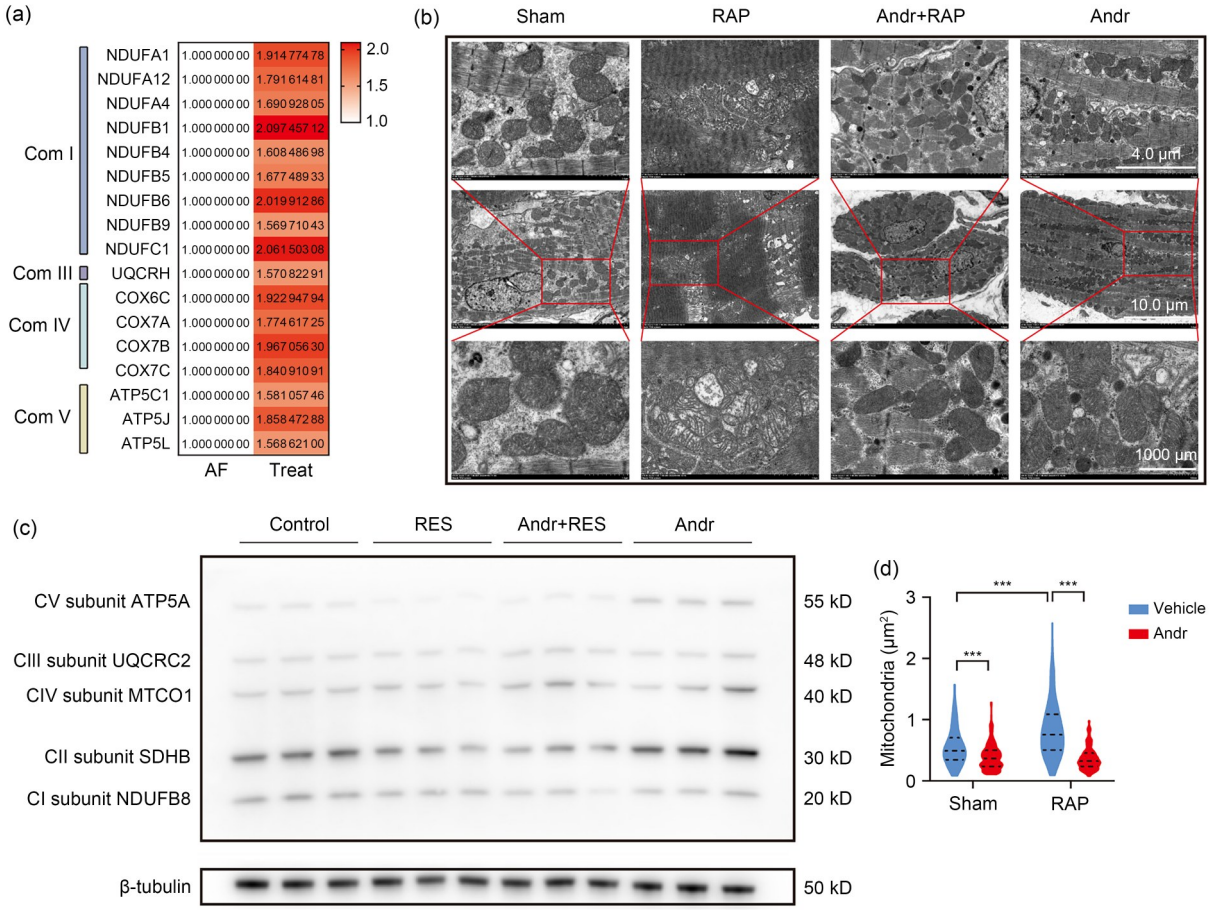

Fig. 10 Effects of andrographolide (Andr) treatment on RAP/RES, inducing atrial myocardial injury by restoring mitochondrial bioenergetics. (a) Contrast chart showing DEGs relevant to the mitochondrial respiratory electron transport chain between the RAP and Andr+RAP groups. The expression of DEGs relevant to the mitochondrial respiratory electron transport chain of the RAP group was defined as 1 (white), and the expression of these genes in the Andr+RAP group was presented as the fold change compared to the RAP group. (b) Representative transmission electron microscopy images of the Sham, RAP, Andr+RAP, and Andr groups. (c) Representative blot images of the protein expression of ETC complex. (d) Quantitative analysis of mitochondrial area. * *P*<0.001. RAP: rapid atrial pacing; RES: rapid electronic stimulation; DEG: differentially expressed gene; ETC: electron transport chain; Com: compound; AF: atrial fibrillation; CI: Compound I; CII: Compound II; CIII: Compound III; CIV: Compound IV; CV: Compound V.**

reduction and increased the AF inducibility and duration, suggesting that Andr treatment resulted in an apparent decrease in AF susceptibility. Meanwhile, Andr treatment effectively shortened the WOV and lengthened the AERP, which hinted that Andr might inhibit the formation of substrate important for AF maintenance. Thus, we further detected whether there were any changes on atrial substrate. However, Masson staining and Sirius Red staining revealed no significant fibrosis among the four groups. The lack of fibrosis suggested that Andr may change the expression of connexin 40 (Cx40) and Cx43; therefore, additional testing was required. During atrial structure remodeling, apart from the atrial fibrosis and the change in the expression of Cx40 and Cx43, the apoptosis of atrial myocytes is important. Thus, we used TUNEL assay and Annexin V/PI staining to evaluate apoptosis in rabbit tissue and HL-1 cells, respectively. Moreover, we detected BAX, BCL2, and cleaved-CASP3 protein expression. We performed RES on HL-1 cells and found reduced protein expression of LCCs and an increase in intracellular ROS production via DHE staining. Additionally, we found that Andr could effectively inhibit apoptosis in vivo and in vitro.

After confirming the effective therapeutic function of Andr on AF, we performed comprehensive RNA-seq analysis to investigate the possible phenotype, BP, and mechanism of Andr. Surprisingly, we found that genes

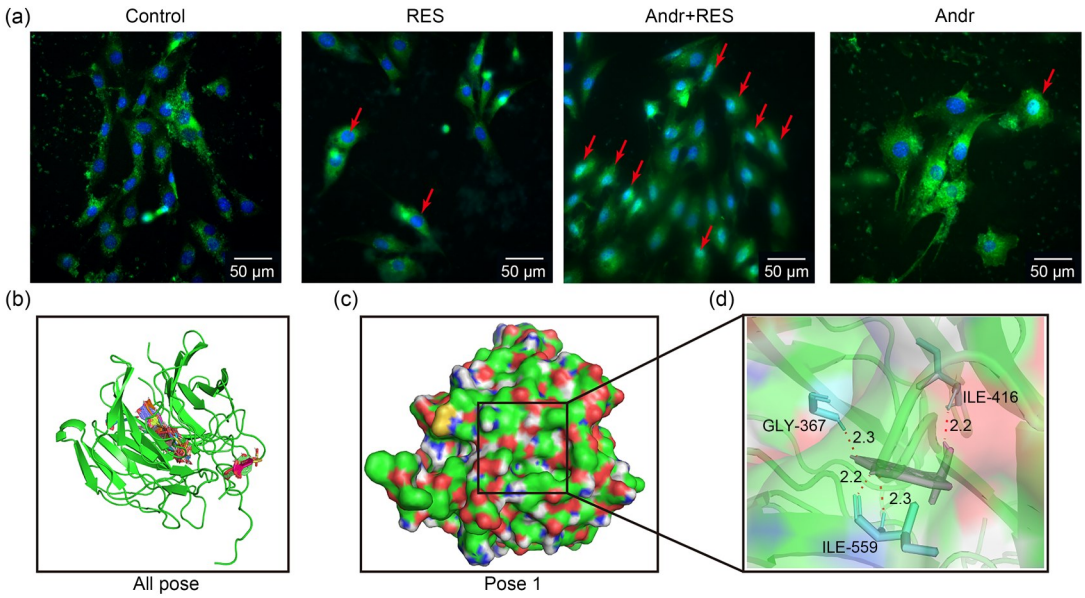

Fig. 11 Effects of andrographolide (Andr) treatment on the development of atrial fibrillation (AF) by influencing the Nrf2-Keap1 complex. (a) Representative images of the translocation of Nrf2 to the nucleus. (b–d) Molecular docking models of Andr binding to the Nrf2-Keap1 complex.

associated with inflammation and the regulation of calcium homeostasis were upregulated. In support of the RNA-seq findings, we conducted ELISA to detect the secretion of TNF-α and IL-1β, in addition to qPCR analysis.

Given that mitochondria are required for the redox balance, intrinsic apoptosis, and intracellular calcium homeostasis, we began to measure the contents of calcium and ROS in the cytoplasm and mitochondria. Transmission electron microscopy analysis suggested that Andr protected atrial myocytes from RAP-induced morphological abnormalities. Furthermore, we carried out proteomics analysis to find that the regulation of many proteins located in the mitochondria were changed significantly. These findings led us to assess the mitochondrial SOD enzymatic activity and total SOD enzymatic activity, and the content of ATP was measured at the cellular level.

PGC-1α is a crucial effector of impaired mitochondrial bioenergetics. Once activated, it can immediately promote the expression of mitochondrial oxidative phosphorylation (OXPHOS)-related proteins. In addition, PGC-1α activates the expression of mitochondrial transcriptional factor A (Tfam), and triggers the transcription and replication of mitochondrial DNA (mtDNA) by the translocation of Tfam into the mitochondria. Moreover, increasing evidence has suggested that HO-1 can positively regulate PGC-1α expression. Shi et al. (2021) confirmed that, by regulating mitochondrial quality control (MQC), HO-1 activation protects from sepsis-induced lung injury. Hull et al. (2016) validated that HO-1 overexpression regulates MQC and promotes mitochondrial biogenesis by Nrf1, PGC-1α, and Tfam upregulation. Herein, we found that PGC-1α and Tfam were downregulated in our AF models both in vitro and in vivo, which could be reversed by Andr. To the best of our knowledge, our study is the first to explore the effect of Andr drug on mitochondria.

The role of PGC-1α and the transcription of HO-1 both depend on transcription factors (TFs). It was reported that by upregulating Nrf2/HO-1, Andr inhibited H_2O_2-induced liver cell death (Mittal et al., 2016). Moreover, others have validated that Andr protects against post-MI damage by promoting the dissociation of Nrf2 from Keap1 and upregulating the expression of HO-1 (Xie et al., 2020). We performed a molecular docking study to find possible key residues where Andr might combine to promote the dissociation of Nrf2 from Keap1 (Fig. 12).

Taken together, our results demonstrated that the preventive effects of Andr on the development of AF and the associated mechanism could contribute to the regulation of mitochondria. Thus, Andr might be a potential drug to treat AF, and anti-oxidant stress response could be a potential target in the clinical prevention of AF.

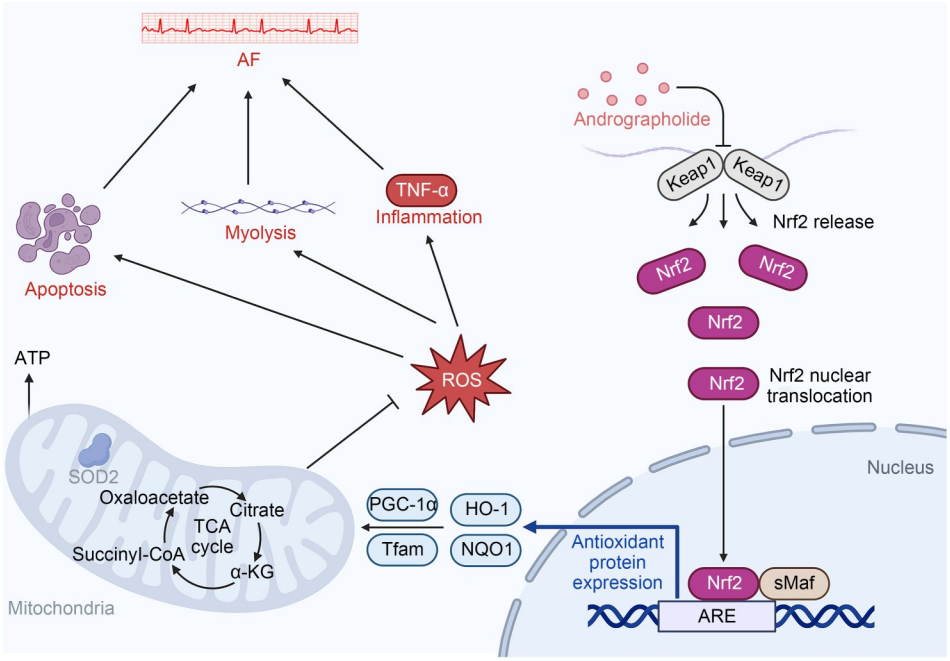

Fig. 12 Therapeutic effect of Andr on AF by Nrf2/HO-1 pathway. Adapted from "Keap1-Nrf2 pathway," from BioRender.com (2020). Retrieved from https://app.biorender.com/biorender-templates. AF: atrial fibrillation; TNF-α: tumor necrosis factor-α; ROS: reactive oxygen species; ATP: adenosine triphosphate; SOD: superoxide dismutase; Tfam: mitochondrial transcriptional factor A; PGC-1α: peroxisome proliferator-activated receptor gamma coactivator 1-α; HO-1: heme oxygenase-1; NQO1: NAD(P)H quinone oxidoreductase 1; Nrf2: nuclear factor erythroid 2-related factor 2; Keap1: Kelch-like ECH-associated protein l; ARE: AU-rich element.

4 Conclusions

The present study highlights Andr as a potential preventive therapeutic drug toward AF via activating HO-1 to promote mitochondrial bioenergetics. Considering the deficiency of using TCM in AF patients, our findings provide novel evidence in support of the therapeutic use of Andr as a TCM.

Materials and methods

Detailed methods are provided in the electronic supplementary materials of this paper.

Acknowledgments

This work was supported by the National Natural Science Foundation of China (No. 82270317) and the Zhejiang Provincial Natural Science Foundation of China (No. LY19H020011).

The authors would like to express gratitude to EditSprings (https://www.editsprings.com) for the expert linguistic services provided.

Author contributions

Conceptualization: Pengcheng YU; Data curation: Pengcheng YU, Jiaru CAO, Huaxin SUN, and Hangying YING; Formal analysis: Pengcheng YU; Investigation: Jiaru CAO and Xinyu ZHOU; Methodology: Pengcheng YU, Jiaru CAO, Huaxin SUN, Yingchao GONG, Qingbo LV, and Hang YANG; Project administration: Ling ZHANG and Xia SHENG; Resources: Xia SHENG; Software: Huaxin SUN, Yingchao GONG, Hangying YING, Yuxing WANG, Chenyang QI, and Hang YANG; Supervision: Ling ZHANG and Xia SHENG; Visualization: Pengcheng YU, Yingchao GONG, Hangying YING, and Yuxing WANG; Writing – original draft: Pengcheng YU; Writing – review & editing: Xia SHENG and Pengcheng YU. All authors have read and approved the final manuscript, and therefore, have full access to all the data in the study and take responsibility for the integrity and security of the data.

Compliance with ethics guidelines

Pengcheng YU, Jiaru CAO, Huaxin SUN, Yingchao GONG, Hangying YING, Xinyu ZHOU, Yuxing WANG, Chenyang QI, Hang YANG, Qingbo LV, Ling ZHANG, and Xia SHENG declare that they have no conflict of interest.

All institutional and national guidelines for the care and use of laboratory animals were followed the Guide for the Care and Use of Laboratory Animals published by the United States National Institutes of Health (NIH publication No. 85-23, revised 1996). This study was conducted with approval by the Institutional Animal Care and Use Committee of the First Affiliated Hospital of Xinjiang Medical University (Approval No. IACUC-20170420-03).

References

Amin A, Houmsse A, Ishola A, et al., 2016. The current approach of atrial fibrillation management. *Avicenna J Med*, 6(1): 8-16.
https://doi.org/10.4103/2231-0770.173580

Brunner G, Abboud L, Shaikh KA, et al., 2012. Left atrial scar burden determined by delayed enhancement cardiac magnetic resonance at post radiofrequency ablation: association with atrial fibrillation recurrence. *J Cardiovasc Magn Reson*, 14(S1):P204.
https://doi.org/10.1186/1532-429x-14-s1-p204

Chen W, Su HM, Feng LN, et al., 2016. Andrographolide suppresses preadipocytes proliferation through glutathione antioxidant systems abrogation. *Life Sci*, 156:21-29.
https://doi.org/10.1016/j.lfs.2016.05.030

Chugh SS, Havmoeller R, Narayanan K, et al., 2014. Worldwide epidemiology of atrial fibrillation: a global burden of disease 2010 study. *Circulation*, 129(8):837-847.
https://doi.org/10.1161/CIRCULATIONAHA.113.005119

Chung MK, Refaat M, Shen WK, et al., 2020. Atrial fibrillation: *JACC* council perspectives. *J Am Coll Cardiol*, 75(14): 1689-1713.
https://doi.org/10.1016/j.jacc.2020.02.025

Dobrev D, Nattel S, 2010. New antiarrhythmic drugs for treatment of atrial fibrillation. *Lancet*, 375(9721):1212-1223.
https://doi.org/10.1016/s0140-6736(10)60096-7

Dong Y, Liao JQ, Yao KW, et al., 2017. Application of traditional Chinese medicine in treatment of atrial fibrillation. *Evid Based Complement Alternat Med*, 2017:1381732.
https://doi.org/10.1155/2017/1381732

Elasoru SE, Rhana P, de Oliveira Barreto T, et al., 2021. Andrographolide protects against isoproterenol-induced myocardial infarction in rats through inhibition of L-type Ca^{2+} and increase of cardiac transient outward K^+ currents. *Eur J Pharmacol*, 906:174194.
https://doi.org/10.1016/j.ejphar.2021.174194

Guo W, Huang JH, Wang N, et al., 2019. Integrating network pharmacology and pharmacological evaluation for deciphering the action mechanism of herbal formula Zuojin pill in suppressing hepatocellular carcinoma. *Front Pharmacol*, 10:1185.
https://doi.org/10.3389/fphar.2019.01185

Hopkins AL, 2008. Network pharmacology: the next paradigm in drug discovery. *Nat Chem Biol*, 4(11):682-690.
https://doi.org/10.1038/nchembio.118

Huang YM, Zhou XM, Liu M, et al., 2020. The natural compound andrographolide inhibits human aortic valve interstitial cell calcification via the NF-kappa B/Akt/ERK pathway. *Biomed Pharmacother*, 125:109985.
https://doi.org/10.1016/j.biopha.2020.109985

Huang YM, Liu M, Liu CG, et al., 2022. The natural product andrographolide ameliorates calcific aortic valve disease by regulating the proliferation of valve interstitial cells *via* the MAPK-ERK pathway. *Front Pharmacol*, 13:871748.
https://doi.org/10.3389/fphar.2022.871748

Hull TD, Boddu R, Guo LL, et al., 2016. Heme oxygenase-1 regulates mitochondrial quality control in the heart. *JCI Insight*, 1(2):e85817.
https://doi.org/10.1172/jci.insight.85817

Kloosterman M, Chua W, Fabritz L, et al., 2020. Sex differences in catheter ablation of atrial fibrillation: results from AXAFA-AFNET 5. *EP Europace*, 22(7):1026-1035.
https://doi.org/10.1093/europace/euaa015

Kumar A, Butler BM, Kumar S, et al., 2015. Integration of structural dynamics and molecular evolution via protein interaction networks: a new era in genomic medicine. *Curr Opin Struct Biol*, 35:135-142.
https://doi.org/10.1016/j.sbi.2015.11.002

Lei YR, Tang Y, Huang L, et al., 2021. Systematic review and meta-analysis on efficacy of traditional Chinese medicine for atrial fibrillation through cluster analysis. *Ann Palliat Med*, 10(8):8982-8990.
https://doi.org/10.21037/apm-21-1785

Li XL, Qiu Q, Li MY, et al., 2021. Chemical composition and pharmacological mechanism of ephedra-glycyrrhiza drug pair against coronavirus disease 2019 (COVID-19). *Aging*, 13(4):4811-4830.
https://doi.org/10.18632/aging.202622

Lin KH, Marthandam Asokan S, Kuo WW, et al., 2020. Andrographolide mitigates cardiac apoptosis to provide cardioprotection in high-fat-diet-induced obese mice. *Environ Toxicol*, 35(6):707-713.
https://doi.org/10.1002/tox.22906

Ma YM, Zhang XZ, Su ZZ, et al., 2015. Insight into the molecular mechanism of a herbal injection by integrating network pharmacology and in vitro. *J Ethnopharmacol*, 173:91-99.
https://doi.org/10.1016/j.jep.2015.07.016

Maiti K, Mukherjee K, Murugan V, et al., 2010. Enhancing bioavailability and hepatoprotective activity of andrographolide from *Andrographis paniculata*, a well-known medicinal food, through its herbosome. *J Sci Food Agric*, 90(1):43-51.
https://doi.org/10.1002/jsfa.3777

Mittal SPK, Khole S, Jagadish N, et al., 2016. Andrographolide protects liver cells from H_2O_2 induced cell death by upregulation of Nrf-2/HO-1 mediated via adenosine A_{2a} receptor signalling. *Biochim Biophys Acta*, 1860(11 Pt A):2377-2390.
https://doi:10.1016/j.bbagen.2016.07.005

Pauklin P, Zilmer M, Eha J, et al., 2022. Markers of inflammation, oxidative stress, and fibrosis in patients with atrial fibrillation. *Oxid Med Cell Longev*, 2022:4556671.
https://doi.org/10.1155/2022/4556671

Ruan XF, Ju CW, Shen Y, et al., 2018. Suxiao Jiuxin pill promotes exosome secretion from mouse cardiac mesenchymal stem cells *in vitro*. *Acta Pharmacol Sin*, 39(4):569-578.
https://doi.org/10.1038/aps.2018.19

Shi J, Yu TX, Song K, et al., 2021. Dexmedetomidine ameliorates endotoxin-induced acute lung injury in vivo and in vitro by preserving mitochondrial dynamic equilibrium through the HIF-1a/HO-1 signaling pathway. *Redox Biol*, 41: 101954.
https://doi.org/10.1016/j.redox.2021.101954

Su HM, Mo JL, Ni JD, et al., 2020. Andrographolide exerts antihyperglycemic effect through strengthening intestinal

barrier function and increasing microbial composition of *Akkermansia muciniphila*. *Oxid Med Cell Longev*, 2020: 6538930.
https://doi.org/10.1155/2020/6538930

Tan YQ, Jin M, He XH, et al., 2022. Huoxue Qingre decoction used for treatment of coronary heart disease network analysis and metabolomic evaluation. *Front Pharmacol*, 13:1025540.
https://doi.org/10.3389/fphar.2022.1025540

Wang M, Xiong H, Lu L, et al., 2022. Serum lipopolysaccharide is associated with the recurrence of atrial fibrillation after radiofrequency ablation by increasing systemic inflammation and atrial fibrosis. *Oxid Med Cell Longev*, 2022: 2405972.
https://doi.org/10.1155/2022/2405972

Wang ZS, Tang Z, Zhu WQ, et al., 2017. Efficacy and safety of traditional Chinese medicine on thromboembolic events in patients with atrial fibrillation: a systematic review and meta-analysis. *Complement Ther Med*, 32:1-10.
https://doi.org/10.1016/j.ctim.2017.03.006

Wu QQ, Ni J, Zhang N, et al., 2017. Andrographolide protects against aortic banding-induced experimental cardiac hypertrophy by inhibiting MAPKs signaling. *Front Pharmacol*, 8:808.
https://doi.org/10.3389/fphar.2017.00808

Xie SY, Deng W, Chen JJ, et al., 2020. Andrographolide protects against adverse cardiac remodeling after myocardial infarction through enhancing Nrf2 signaling pathway. *Int J Biol Sci*, 16(1):12-26.
https://doi.org/10.7150/ijbs.37269

Ye SJ, Luo W, Khan ZA, et al., 2020. Celastrol attenuates angiotensin ii-induced cardiac remodeling by targeting STAT3. *Circ Res*, 126(8):1007-1023.
https://doi.org/10.1161/CIRCRESAHA.119.315861

Zeng ML, Jiang WZ, Tian YJ, et al., 2017. Andrographolide inhibits arrhythmias and is cardioprotective in rabbits. *Oncotarget*, 8(37):61226-61238.
https://doi.org/10.18632/oncotarget.18051

Zhan SK, Liang JY, Lin HT, et al., 2023. SATB1/SLC7A11/HO-1 axis ameliorates ferroptosis in neuron cells after ischemic stroke by Danhong injection. *Mol Neurobiol*, 60(1):413-427.
https://doi.org/10.1007/s12035-022-03075-z

Zhang L, Po SS, Wang H, et al., 2015. Autonomic remodeling: how atrial fibrillation begets atrial fibrillation in the first 24 hours. *J Cardiovasc Pharmacol*, 66(3):307-315.
https://doi.org/10.1097/FJC.0000000000000281

Supplementary information

Tables S1–S3; Fig. S1; Materials and methods